Amplification of a high-order harmonic pulse in an active medium of a plasma-based x-ray laser

Chul Min Kim, Karol A. Janulewicz,* Hyung Taek Kim, and Jongmin Lee†
Center for Femto-Atto Science and Technology, and Advanced Photonics Research Institute, Gwangju Institute of Science and Technology, Gwangju 500-712, Korea
(Received 24 April 2009; published 10 November 2009)

We investigate theoretically amplification of a high-order harmonic pulse in an active medium of x-ray laser. Using a model based on Maxwell-Bloch equations, which are modified to incorporate time-dependent gain and statistical character of spontaneous emission, the time-dependent nature of the interaction including coherent process is studied. The temporal shape of the output pulse is found to consist of three components: amplified spontaneous emission, coherent transient phase, and coherent decay. Based on this analysis, energy extraction and duration of the output pulse are discussed. The expectation regarding the properties such as radiation polarization, coherence, and divergence is also considered.

DOI: 10.1103/PhysRevA.80.053811 PACS number(s): 42.55.Vc, 42.50.Md, 42.65.Ky

High harmonics (HHs) and x-ray lasers (XRLs) are the two representative coherent extreme ultraviolet (euv) sources of very different characteristics [1]. HH provides a broadband linearly polarized and almost fully coherent frequency comb. Its spectrum covers the wavelength from that of the driving optical laser to its hundredth harmonics, and the duration of a single pulse is usually between few tens of fs and sub-fs. However, the energy of a single harmonic order is low and varies between pJ and sub-μJ. In contrast, randomly polarized radiation of XRL provides an extremely narrow ($\Delta\lambda/\lambda \leq 10^{-4}$) spectrum and is only partially coherent (1–3 %). The emitted pulse has a duration of several ps, and an energy of few μJ, in the case of compact devices.

The idea of injecting a HH pulse into an x-ray laser active medium to realize a strong ultrashort coherent euv source with well-defined polarization has been conceived from the burgeoning period of HH research. In this way, the advantages of HH may be mapped on the output pulse [2]. The first experiment trying to realize this scheme gave low gain of around 3 affected by inefficient seed generation [3]. However, a decade later, with progress in both HH and XRL, saturated amplification was achieved with both gas target XRL [4] and solid target XRL [5]. Very recently, various parameters of the output pulse generated by seeding, e.g., coherence, divergence, and pulse duration, have been investigated in detail [6,7].

The achievement of gain saturation by seeding the optical-field-ionized x-ray lasers was concluded with the expectation of fully coherent fs pulses of mJ energy in the nearest future [4]. However, the subsequent experiments using the state-of-the-art HH seeders and amplifying media failed to achieve this promised level of the output parameters [6–8], and the question arouse about the origin of the observed limited output. After an extensive numerical simulation incorporating plasma dynamics of lasing medium, it was reported that there exists "an intrinsic difficulty on the way to truly femtosecond XRLs through the amplification of short [high-order harmonics] pulses, namely, the fact that the laser tends to operate over its natural time scale of order $1/\gamma$ rather than the incident pulse time scale" [9], in other words, the amplifying medium of the XRL is inherently resistant to the expected amplification process.

In the present paper, we extend the kinetic model used in [9] to explain the physical processes and parameters which are responsible for amplification and the character of the limited output observed in the experiment. Because the HH pulsewidth (tens of femtoseconds) is much shorter than the dipole relaxation time of the lasing medium (subpicoseconds), the coherent and time-dependent nature of the interaction should be fully incorporated. Thus, Maxwell-Bloch-type equations are used to describe the pulse propagation and kinetic processes in the amplifying medium [10–12]. The properties of the amplifying medium were incorporated by fixed relaxation rates, fixed electron density, and time-dependent gain. For simplicity, the medium was assumed to satisfy the condition of ideal traveling wave amplification, and interaction had resonant character. Uniform beam cross section of area 400 μm^2 was also assumed. Further simplification used to make the physics behind the amplification process more intuitive was using one-dimensional (1D) geometry or a sort of uniform medium approximation, regardless of very complex propagation in the plasma plume. The resulting equations (applying atomic unit system) have the following form:

$$\partial P/\partial \tau = -\gamma_{ba} P - i z_{ba}^2 E\{N_b - N_a\} + \Gamma,$$

$$\partial N_b/\partial \tau = -\gamma_b N_b + \mathrm{Im}\{E^* P\}/2 + R_b,$$

$$\partial N_a/\partial \tau = -\gamma_a N_a - \mathrm{Im}\{E^* P\}/2 + \gamma_{br} N_b,$$

$$\partial E/\partial y = (i 2\pi\omega_0/c)(P - n_e E/\omega_0^2).$$

The equations of polarization (P), upper state population (N_b), and lower state population (N_a) describe material response, and the last equation is the wave equation for electric field (E). These quantities are functions of propagation length (y) and reduced time ($\tau = t - y/c$). P and E refer to the

*Also at School of Photon Science and Technology, Gwangju Institute of Science and Technology, Gwangju 500-712, Korea; kaj@gist.ac.kr
†leejm@gist.ac.kr

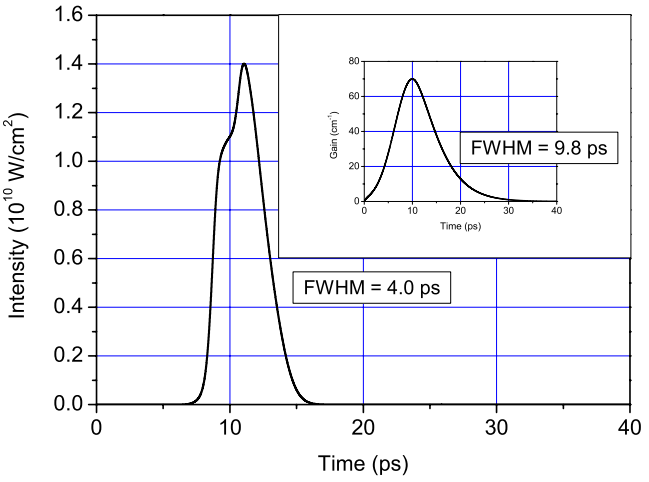

FIG. 1. (Color online) Temporal profile of the XRL pulse from 4-mm-long medium (FWHM=4.0 ps). The inset shows the temporal gain profile of the lasing medium (FWHM=9.8 ps), of which maximum is 70 cm^{-1}.

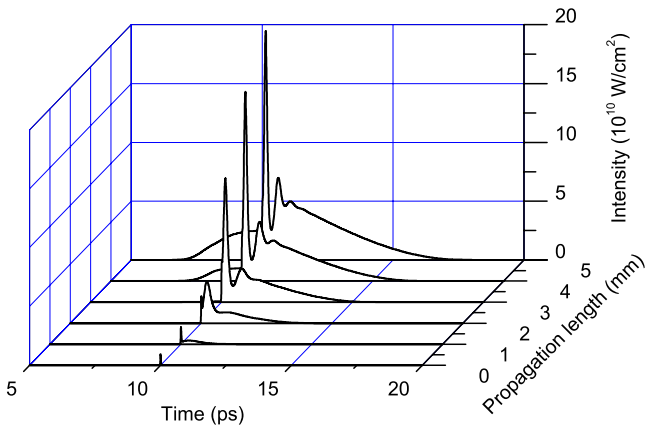

FIG. 2. (Color online) Evolution of harmonic pulse as it propagates through the lasing medium, of which gain is as shown in the inset of Fig. 1

complex amplitudes of the corresponding physical quantities [13]. $\Gamma(N_b,\tau)$ is a random source term representing spontaneous emission [12,14], and $R_b(\tau)$ is a pumping term simulating time-dependent gain or population of the upper state. The parameters and pumping term chosen to simulate $4d(^1S_0)\rightarrow 4p(^1P_1)$ transition in Ag^{19+} were obtained either from simulations or from experimental data quoted in the literature: $\hbar\omega_0=89$ eV, dipole relaxation rate $\gamma_{ba}=3.4\times10^{12}$ Hz corresponding to $\Delta\lambda/\lambda=5\times10^{-5}$, and $n_e=2\times10^{20}$ cm^{-3} from typical experimental results [1]; radiative decay rate $\gamma_{br}=5.9\times10^{10}$ Hz and dipole matrix element $z_{ba}=0.27$ au from MCDFGME (see [15]); upper state decay rate $\gamma_b=2.6\times10^{12}$ Hz, and lower state decay rate $\gamma_a=2.3\times10^{12}$ Hz from EHYBRID [16]. Although the real system involves two levels consisting of four states due to the degeneracy of the lower level, and radiation polarization is two-dimensional [17], the current model should produce the correct qualitative behavior of the real system [12].

The output pulse from a conventional XRL was obtained by using the above set of equations, as shown in Fig. 1. It depicts the temporal profile of the pulse generated by 4-mm-long lasing medium, of which time-dependent small-signal gain is shown in the figure inset. The maximum value of the gain is 70 cm^{-1}, and the gain duration is 9.8 ps [full width at half maximum (FWHM)]. The energy and pulse width of the output pulse are 220 nJ and 4.0 ps, respectively. These values are in reasonable agreement with experimental reports [18,19]. The pulse grows from the noise of spontaneous emission (described by Γ in the first equation), and the resulting pulse duration (4.0 ps) is comparable to the gain duration (9.8 ps). Although the pulse is initially weak and noiselike, it develops into a strong partially coherent pulse due to the resonant interaction. The rising edge is steeper than the falling edge because of the asymmetry in the amplification process. The current model employing 1D geometry and only two atomic states cannot describe radiation polarization, coherence, and divergence properly, but it is assumed that this pulse has random polarization and is less coherent and more divergent than a HH pulse, which is emitted from the atoms driven by a fully coherent optical laser pulse.

When a HH pulse is injected into the amplifying medium, the profile of the output pulse becomes entirely different. The propagation of a 25 fs 1 nJ HH pulse, which is arriving at the gain peak, is depicted in Fig. 2. Although the energy of the incident seeding HH pulse is just 1 nJ, its intensity is so high due to the short duration that a significant polarization is immediately developed in the medium. This polarization, decaying on the time scale of dipole dephasing time $(1/\gamma_{ba}=0.29$ ps), emits at early stages of the medium resonant radiation which trails the input HH pulse, as seen from the pulse shape at 1 mm. This combination of HH pulse and its trailer constitutes a seeder for the later stages of the medium. In further propagation, the trailing part is amplified so much that the oscillatory pulse shape, i.e., coherent transient phase [10], is achieved, as seen from the pulse shape at 2 mm. The modulation in field intensity is the result of Rabi oscillation of the populations between the two atomic states, and it clearly shows that the radiation is sufficiently strong to control population dynamics. In this phase of the pulse development, the contribution to the polarization from spontaneous emission is negligible, which means that such a pulse should be highly coherent. Furthermore, the radiation polarization will be that of the HH pulse, i.e., linear polarization, and the divergence will be reduced. The part that trails the oscillation should also have these properties because it is the result of polarization decay. As the pulse propagates over longer distances, the amplified spontaneous emission (ASE) of a noticeable level is developed in front of the amplified HH pulse, as seen from the profiles at 4 mm and onward. This ASE part should have the properties of the conventional XRL pulse: random polarization, low coherence, and significant divergence. Hence, the output pulse of the amplifier consists of three distinguishable parts: ASE, coherent transient phase, and coherent decay.

The detailed feature of the induced Rabi oscillation is depicted in Fig. 3. The short spike at $t=10$ ps is a result of the modest amplification of the input HH pulse, but the following oscillatory and decay parts contain a significant part

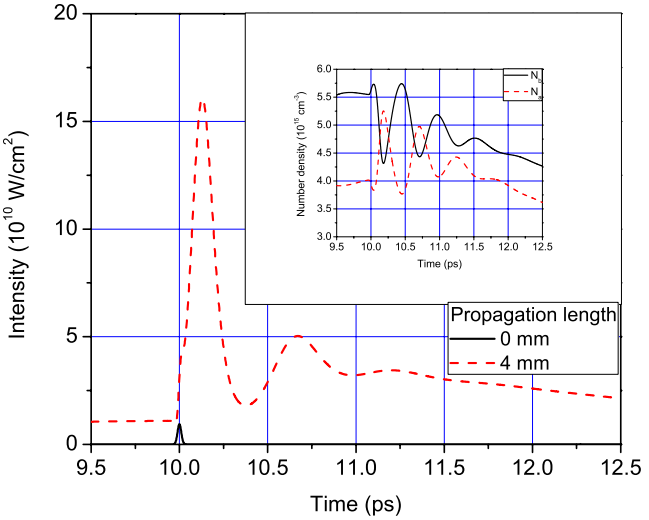

FIG. 3. (Color online) Temporal profile of the input HH pulse and the amplified pulse after 4 mm propagation. Input HH energy is 1 nJ. The main peak of the temporal profile at 4 mm has the pulsewidth of 0.15 ps. The inset shows the population variation of upper and lower states at 4 mm.

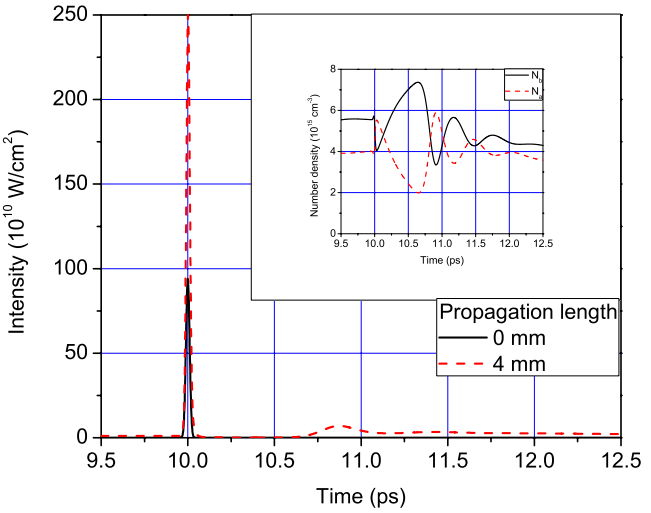

FIG. 4. (Color online) Temporal profile of the input HH pulse and the amplified pulse after 4 mm propagation. Input HH energy is 100 nJ. The main peak of the temporal profile at 4 mm has the pulse width of 25 fs. The inset shows the population variation of upper and lower states at 4 mm.

of the total pulse energy. In this case, the pulse width of the main peak is 0.15 ps (FWHM), which is shorter than the relaxation time of the active medium but much longer than the pulse width of the input HH pulse. The pulse width calculated as root mean square deviation (RMSD) equals to 1.5 ps due to the long pedestal consisting of ASE and the decay component. The output pulse energy is 560 nJ, and hence the total amplification is 560. The accompanying population dynamics is shown in the inset of Fig. 3. It is clear and important to note that the input HH only initiates coherent transient phase and is hardly amplified.

When the incident HH energy increases to 100 nJ, the temporal profile becomes different, and amplification is reduced due to immediate saturation. As shown in the inset of Fig. 4, the HH pulse itself is sufficiently strong to invert the existing population instantaneously—the medium becomes suddenly absorptive. Consequently, the electric field after the HH pulse remains very weak until the sufficient energy is stored in upper state and subsequently is given to the field. The main peak, which contains significant part of the pulse energy, has a pulse width of 25 fs, i.e., the pulse width of the input HH pulse. This peak is followed, after a significant delay, by the decay phase at noticeably lower level. Provided that the pulse width is the shorter than the relaxation rates, such a scenario can be explained in terms of pulse area $[\theta = ez_{ba}\int E(t)dt/\hbar]$. The pulse area for the 100 nJ pulse is 0.7π while for the 1 nJ pulse 0.07π. If the area of the pulse approaches the value of π, this pulse will rapidly invert the population within its duration. This can be treated as an arbitrarily chosen criterion for oversaturated amplification. As in the case of 1 nJ, the pulse width (RMSD) is 1.5 ps due to the much weaker but long pedestal of ASE and the coherent decay. The output pulse energy is 690 nJ, and the amplification factor is 6.9. In contrast to the previous case, the degree of amplification is greatly decreased while the pulse width of the main peak is shortened. As shown in Fig. 5, gain saturation occurs on shorter propagation length as the input energy increases. In extreme cases of very high level of the injected pulse, the output energy is linearly dependent on the propagation length from the beginning-the signature of oversaturation.

From Fig. 5, the saturated output of seeded XRL seems to be close to that of the conventional ASE XRL, if the input pulse energy is not extremely high. This aspect needs a comment. Actually, in the conducted experiments, the energy extraction with seeding has been observed to be lower than that with ASE only. In the figure, the rate of energy enhancement for ASE XRL is higher than that of seeded XRL: to achieve 100 nJ from the level of 1 nJ, ASE XRL needs only 1.1 mm while the XRL seeded with 1 nJ HH pulse needs 1.9 mm. The reason for this is that a 1 nJ ASE pulse developed from long-lasting spontaneous emission can exploit the whole du-

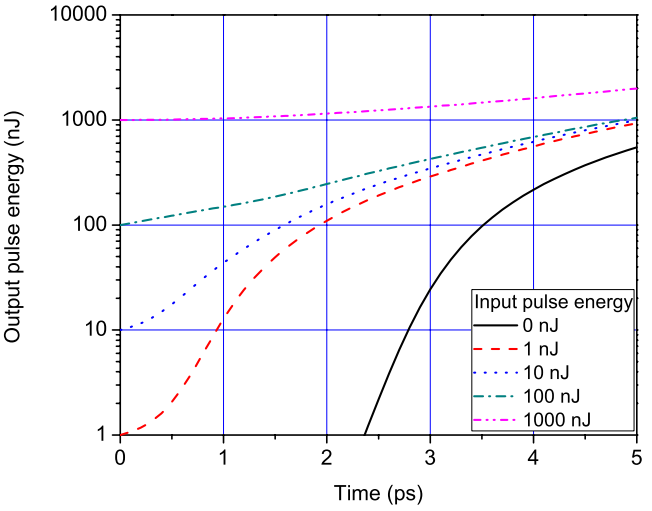

FIG. 5. (Color online) Output pulse energy vs propagation length. The input HH pulse energy is varied from 0 to 1000 nJ.

ration of gain. However, the seeded XRL mostly exploits the gain around its peak at its early stages, and the energy exchange between atom and radiation due to stronger Rabi oscillation limits energy extraction. In the real experiments, a quite nonuniform medium is ordinarily obtained, and some local strengthening of the signal can be expected, and then the output pulse of ASE XRL can quickly exceed the energy of the seeded signal due to higher amplification rate. As a result, the advantage of seeding in terms of energy extraction can be modest in the usual experimental condition.

In conclusion, the HH seeding is still a reasonable technique to realize a strong ultrashort coherent euv source with linear polarization and improved beam qualities. As inferred from the temporal shape, the peak intensity of the output pulse can be strengthened compared to that of the ASE XRL. The width of the main peak pulse can be shorter than 1 ps although the accompanying pedestal exceeds 1 ps. The increase of coherence, reduction of divergence, and accomplishment of linear polarization are expected, even if not included in the current model. Most of these properties have already been experimentally verified [6]. Finally, the geometry of pumping and propagation used in the model is simplified, and one should be cautious comparing the results directly with the experimental data. The existing density gradients and influence of gain factor on refraction index can cause noticeable distortion of the pulse profile leading to smearing effect.

We appreciate Professor G. J. Pert for providing EHYBRID code and invaluable discussion, Dr. P. V. Nickles and Professor J. J. Rocca for important and comprehensive comments on the paper, and Dr. P. Indelicato for providing MCDFGME code. This work was supported by the Ministry of Knowledge and Economy of Korea through the Ultrashort Quantum Beam Facility Program, by the Korea Foundation for International Cooperation of Science and Technology (KICOS) through a grant provided by the Korean Ministry of Education, Science and Technology (MEST) in 2008 (Grant No. K20821000002-08B1200-00210, Korea-Germany collaboration project), and also by Basic Science Research Program through the National Research Foundation of Korea (NRF) funded by MEST (Grant No. R15-2008-006-03001-0).

[1] P. Jaeglé, *Coherent Sources of XUV Radiation: Soft X-Ray Lasers and High-Order Harmonic Generation* (Springer, New York, 2005).
[2] J. Costello, Nat. Photonics **2**, 67 (2008).
[3] T. Ditmire *et al.*, Phys. Rev. A **51**, R4337 (1995).
[4] Ph. Zeitoun *et al.*, Nature (London) **431**, 426 (2004).
[5] Y. Wang, E. Granados, M. A. Larotonda, M. Berrill, B. M. Luther, D. Patel, C. S. Menoni, and J. J. Rocca, Phys. Rev. Lett. **97**, 123901 (2006).
[6] Y. Wang *et al.*, Nat. Photonics **2**, 94 (2008).
[7] Y. Wang, M. Berrill, F. Pedaci, M. M. Shakya, S. Gilbertson, Z. Chang, E. Granados, B. M. Luther, M. A. Larotonda, and J. J. Rocca, Phys. Rev. A **79**, 023810 (2009).
[8] F. Pedaci *et al.*, Opt. Lett. **33**, 491 (2008).
[9] I. R. Al'miev, O. Larroche, D. Benredjem, J. Dubau, S. Kazamias, C. Moller, and A. Klisnick, Phys. Rev. Lett. **99**, 123902 (2007).
[10] J. I. Steinfeld, *Molecules and Radiation*, 2nd ed. (Dover, New York, 2005).
[11] E. Armandillo and I. J. Spalding, J. Phys. D **8**, 2123 (1975).
[12] O. Larroche, D. Ros, A. Klisnick, A. Sureau, C. Moller, and H. Guennou, Phys. Rev. A **62**, 043815 (2000).
[13] M. Born and E. Wolf, *Principles of Optics*, 7th ed. (Cambridge University Press, Cambridge, England, 2005).
[14] S. Chandrasekhar, Rev. Mod. Phys. **21**, 383 (1949).
[15] MCDFGME, (MultiConfiguration Dirac Fock and General Matrix Elements program, release 2005) written by J. P. Desclaux and P. Indelicato (http://dirac.spectro.jussieu.fr/mcdf).
[16] G. J. Pert, J. Fluid Mech. **131**, 401 (1983).
[17] N. Hasegawa *et al.*, J. Opt. Soc. Korea **13**, 60 (2009).
[18] Y. Wang, M. A. Larotonda, B. M. Luther, D. Alessi, M. Berrill, V. N. Shlyaptsev, and J. J. Rocca, Phys. Rev. A **72**, 053807 (2005).
[19] H. T. Kim *et al.*, Phys. Rev. A **77**, 023807 (2008).